FOSSEE Case study project
November 8, 2019

Effect of transverse magnetic field on the conducting fluid flow through pipe with constriction

Padmini Priyadarshini Sivaraj

1

November 8, 2019

ABSTRACT

The influence of transverse magnetic field on the electrically conducting fluid flow through a channel with a constriction in the middle is studied using OpenFOAM. The effects of the Reynolds number and Hartmann number on the flow parameters are discussed. Numerical simulations are performed using mhdFoam, an OpenFOAM solver for incompressible MHD flow. The flow is investigated at three different Reynolds number (Re = 50, 100, 150), and four different Hartmann number (Ha = 0, 10, 20, 30) keeping the Reynolds number and the magnetic Reynolds number constant.
It is found that the magnetic field has a controlling effect on the separation zone: as the Hartmann number is increased, the length of the separation zone is observed to decreases. However, this controlling effect of the electromagnetic field comes with the price of an increase in pressure drop.

Key words. MHD – Flow through constriction – OpenFOAM

1. Introduction

Magnetohydrodynamics deals with the behaviour of the flow of electrically conducting fluid in the electromagnetic field. Magnetohydrodynamics has wide application in geophysics, astrophysics, engineering and medical field. The study of MHD flow inside channels and pipe are rudimentary in engineering applications like in metallurgical industries, nuclear fusion reactor and MHD power generators. And, in many such applications, devices like orifices, valves and nozzles are present. These devices are often used to reduce the pressure or to reduce the flow rate or used as a flow measurement devices. Hence, the study of MHD flow through such constricted passage forms a basis for these engineering and scientific application.

The method of controlling flow separation using electromagnetic forces is also a long-discussed topic. The technique of controlling the flow separation on hydrofoils using electromagnetic force was investigated by Weier et al. (2003)

Midya et al. (2003) studied the steady, incompressible, viscous and electrically conducting flow through a channel with local symmetric constriction with a shape given by Gaussian distribution $y = \frac{w}{2} - d \times e^{-\left(\frac{4(x-x_0)}{H}\right)}$ and obtained numerical solution for such flows. A similar problem was numerically examined using D2Q9 lattice model and the effect of different Reynolds number, magnetic Reynolds number, and Hartmann number were also studied by Ghahderijani et al. (2017)

In the present work, the same case setup mentioned by Midya et al. (2003) is solved numerically using OpenFOAM and the effect of Reynolds number, and Hartmann number on flow separation zone are discussed.

2. Problem definition

We consider a steady, incompressible, laminar, viscous, electrically conducting fluid flow inside a channel of length, L and width, H with the symmetric constriction of height, d placed in the middle of the channel. The shape of the constriction is assumed to be Gaussian function Ghahderijani et al. (2017). A uniform magnetic field of strength B is applied perpendicular to the flow direction. The walls are assumed to be perfectly conducting Hartmann walls. The setup is shown in Figure 1

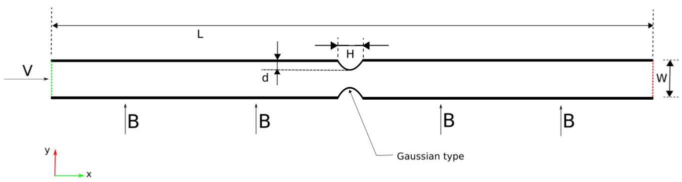

Fig. 1: Case Setup

The geometry consists of three parts 1) the inlet 2) the outlet, and 3) the wall. The boundary conditions for the model are presented in the table 1

Geometric details are: Length of the channel, L = 8 m ; Width of the channel, w = 0.5 m ; Width of the constriction, H = 0.4 m ; Height of the constriction, d = 0.125 m

Physical properties of the working fluid are as follows: Density, $\rho = 1\ kg/m^3$; Magnetic constant, $\mu_0 = 1\ H/m$; Electrical conductivity, $\sigma = 10\ S/m$

The values of dynamic viscosity are varied for simulating flows at different Reynolds number.

The simulations are run at three different dynamic viscosity, $\mu = 0.01\ kg/ms$, $0.015\ kg/ms$, $0.03\ kg/ms$.

Table 1: Boundary conditions

	Pressure $(Pascal)$	Velocity (m/s)	Magnetic Field $(Tesla)$	pB $(Teslam/s)$
Inlet	$\partial P/\partial z = 0$	(0 0 3)	(0 0 0)	0
Outlet	0	$\partial V/\partial z = 0$	(0 0 0)	0
Wall	$\partial P/\partial n = 0$	$\partial V/\partial n = 0$	$(0\ B_y\ 0)$	0

The fundamental equation governing the steady, incompressible, viscous, magnetohydrodynamic flow is given by the following equation.

1) Conservation of mass

$$\nabla.\mathbf{V} = 0 \tag{1}$$

2) Conservation of momemtum

$$\frac{\partial \mathbf{V}}{\partial t} + \nabla.(\mathbf{VV}) - \nabla.\left(\frac{1}{\mu_0\rho}\mathbf{BB}\right) - \nu\Delta\mathbf{V} + \nabla\left(\frac{1}{2\mu_0\rho}B^2\right) = -\nabla P \tag{2}$$

3) Conservation of magnetic flux

$$\nabla.\mathbf{B} = 0 \tag{3}$$

4) Magnetic induction equation

$$\frac{\partial \mathbf{B}}{\partial t} + \nabla.(\mathbf{VB}) - \nabla.(\mathbf{BV}) - \Delta\left(\frac{1}{\mu_0\sigma}\mathbf{B}\right) = 0 \tag{4}$$

The Reynolds number, magnetic Reynolds number, and Hartmann number are defined as follows:

1. Reynolds number

$$\frac{Inertial force}{Viscous force} = Re = \frac{V_m L_c}{\nu} \tag{5}$$

2. Magnetic Reynolds number

$$\frac{magnetic\ field\ convection}{magnetic\ field\ diffusion} = \frac{\mu_0\sigma(\mathbf{V}\times\mathbf{B})}{\nabla\times\mathbf{B}} \sim Re_m = \frac{V_m L_c}{\eta} \tag{6}$$

where magnetic diffusivity η is defined as the ratio of electrical resistivity to magnetic constant.

3. Hartmann number

$$\frac{Electromagnetic force}{Viscous force} = Ha = BL_c\sqrt{\frac{\sigma}{\mu}} \tag{7}$$

where L_c, V_c refers to the characteristic length and characteristic velocity respectivity and in this case L_c = Diameter of the pipe and V_c = Velocity at the inlet.

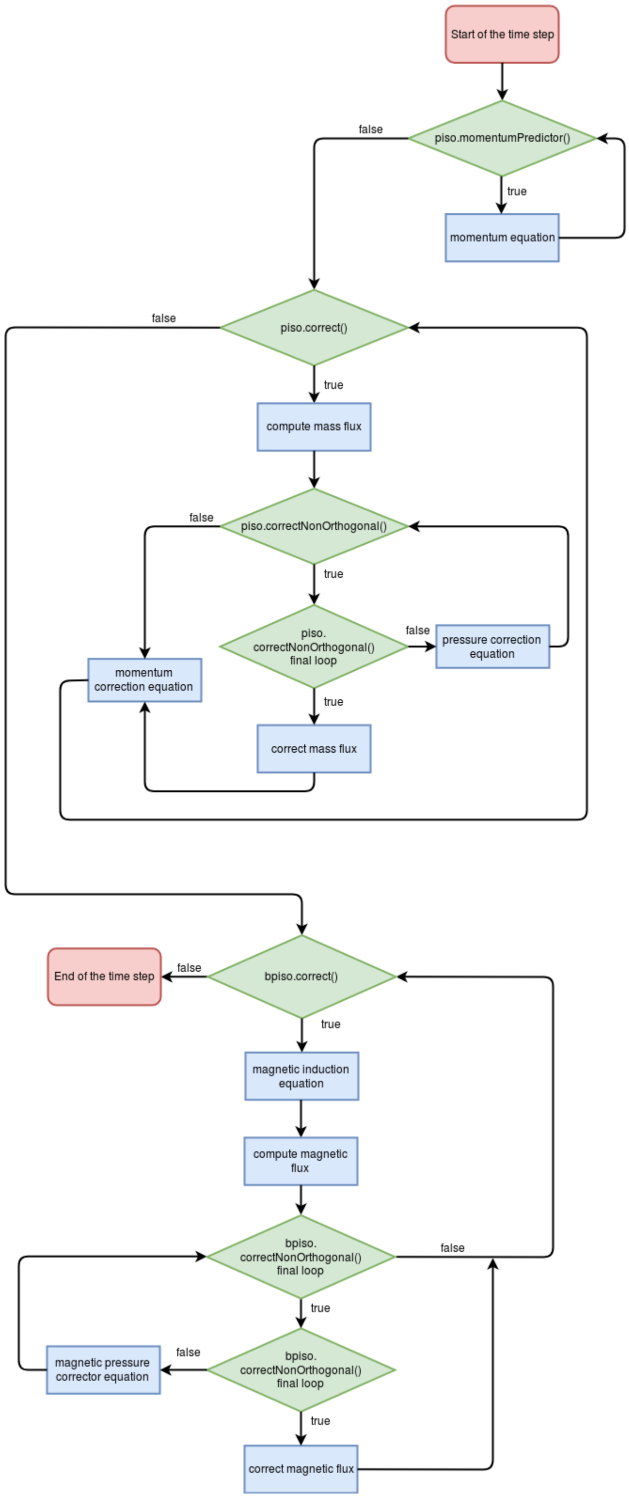

Fig. 2: mhdFoam solver algorithm

The mhdFoam, a pressure-based solver, is an OpenFOAM solver that uses magnetic induction method to solve the MHD equations. This solver solves the governing equations using the PISO algorithm. The magnetic induction equation is solved using PISO algorithm in a similar manner it is implemented in solving the Navier-strokes equation. Figure 2 shows the detailed flowchart.

3. Mesh and grid Independence

The geometry is meshed using Gmsh, finite-element mesh generator. Grid independence study is conducted for two different meshes. The detail of the meshes are shown in the table.

Table 2: Mesh Details

	Section 1	Section 2	Section 3
Mesh no. 1	90 × 25	25 × 25	90 × 25
Mesh no. 2	180 × 50	50 × 50	180 × 50

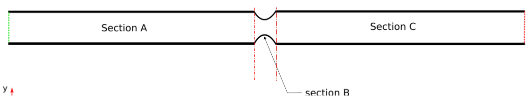

From the graphs 3 and 4, it is observed that the velocity and pressure are in good agreement for different meshes. Mesh number 1 is used for further simulations.

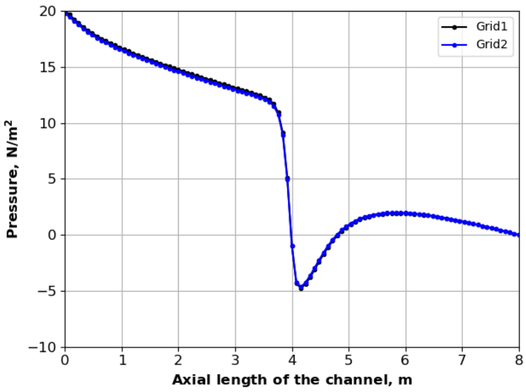

Fig. 3: Axial variation of pressure

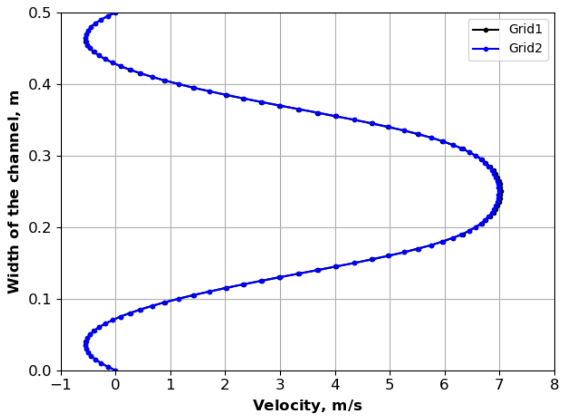

Fig. 4: Widthwise velocity profile at x = 4.2 cm

The 5 shows the region near constriction. As can be seen in the figure, the mesh is refined near the wall to capture the boundary layer and the number of cells in and near the constriction region is relatively high.

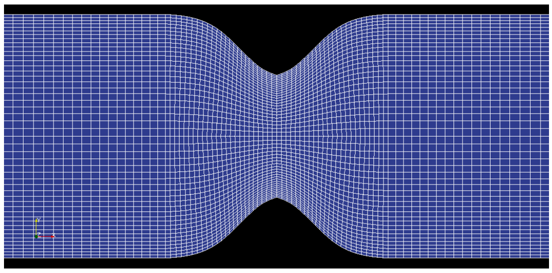

Fig. 5: Mesh

4. Result and Discussion

The simulations are at three different Reynolds number (Re = 50, 100, 150) and four different Hartmann number (Ha = 0, 10, 20, 30) keeping Reynolds number and magnetic Reynolds number constant using mesh number 1 with 10848 cells. The results are plotted using matplotlib, python.

Figure 6 shows the streamline pattern of the flows at three different values of viscosity i.e., three different Reynolds numbers. As expected, the recirculation zone length increase with increase in Reynolds number.

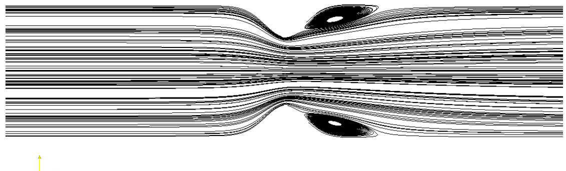

(a) Re = 50

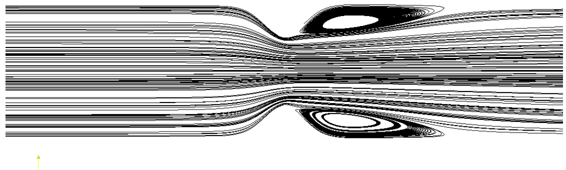

(b) Re = 100

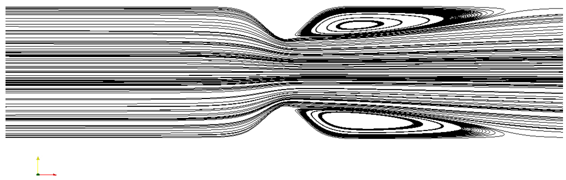

(c) Re = 150

Fig. 6: Streamlines pattern for different Reynolds number

There is a drop in pressure at the throat of the constriction due to Bernoulli's effect: pressure decrease as the flow velocity increase. As the flow enters the diverging portion of the constriction, the flow velocity decreases in the flow direction, and it faces an adverse pressure gradient resulting in the reversal of flow direction. This cause negative flow velocity near the wall of the divergent section. Thus, The negative velocity seen in Figure 8 belongs to the recirculation zone. As the Reynolds number is increased, the viscous force decrease relatively over the inertial force, this decrease the momentum diffusion due to viscosity, which in turn delays the reattachment of flow. As a result, the re-circulation region to grow in size.

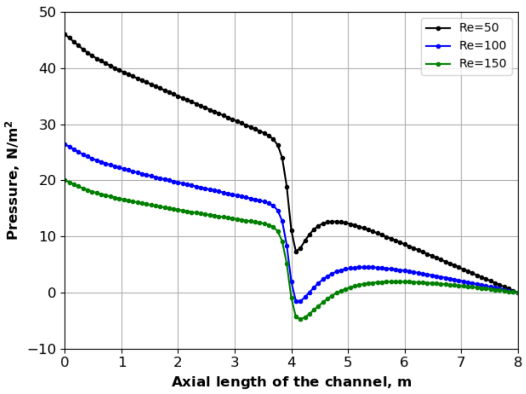

Fig. 7: Axial variation of pressure

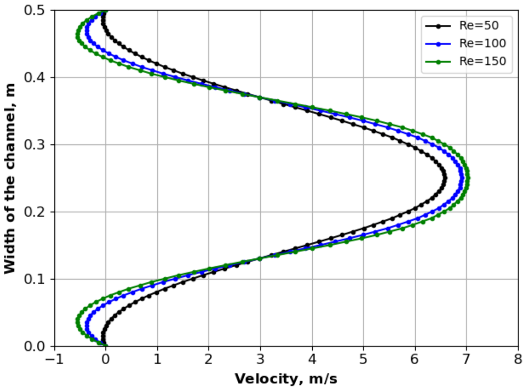

Fig. 8: Widthwise velocity profile at x = 4.2m

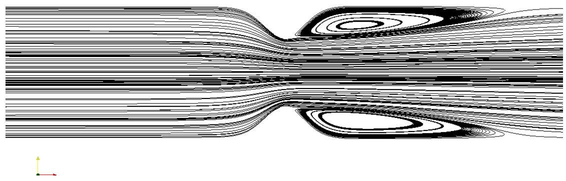

(a) Ha = 0

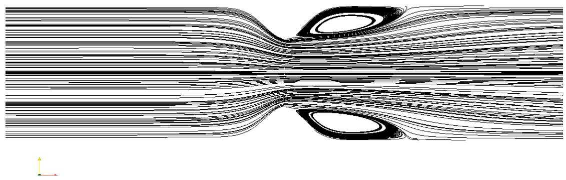

(b) Ha = 10

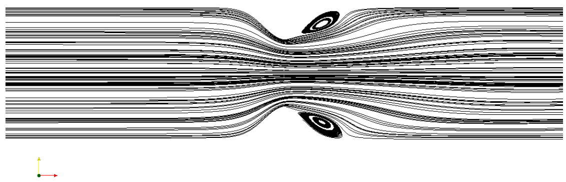

(c) Ha = 20

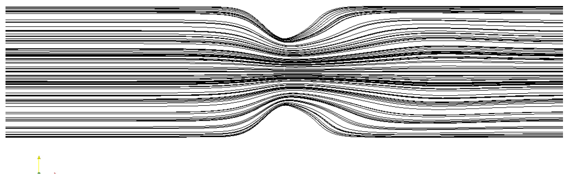

(d) Ha = 30

Fig. 9: Streamlines pattern for different Hartmann number at $Re = 150, Re_m = 15$

It is seen from the Figure 9 that the length of the separation zone decreases as the Hartmann number increases and at certain Hartmann number, the separation zone completely vanishes. These streamline patterns are obtained using the paraView tool called 'streamtracer'.

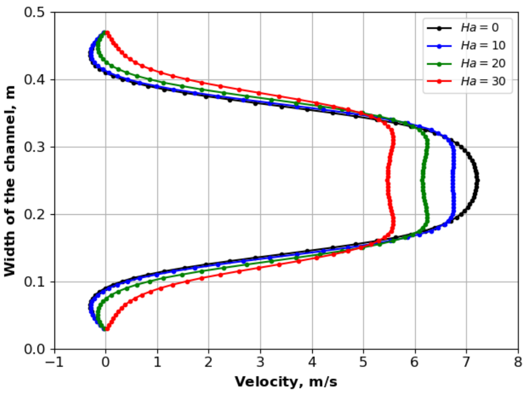

Fig. 10: Widthwise velocity profile at x = 4.125m

The Figure 10 shows that the widthwise velocity profile becomes flatter. The Lorentz force generated by the interaction between the applied and the induced magnetic field retards the flow near the pipe axis; to keep the mass flow rate constant, the flow near the wall must accelerate. This acceleration near the wall increases with increase in the applied magnetic field strength. The accelerated boundary layer flow suppresses the flow reversal and encourage the reattachment of the flow.

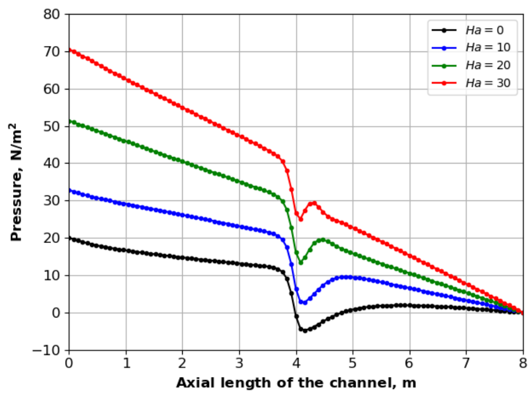

Fig. 11: Axial variation of pressure

The increased velocity near the wall results in increased wall shear stress (see Figure). The axial pressure drop increase as wall shear stress increases: to push the same amount of flow more work is needed to overcome the increased shear on the wall. Hence, the Figure 11 shows an increasing pressure difference for increasing Hartmann number at a constant Reynolds number.

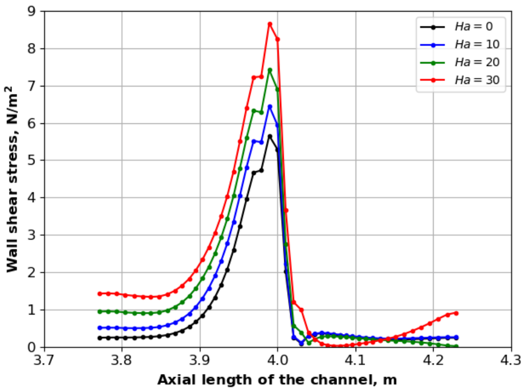

Fig. 12: Wall shear stress in the constriction region

As the Hartmann number increases, the flow in the diverging portion of the constriction is attached to the wall for slightly longer distance. This effect can be seen the Figure 12 at approximately 4.02 *m*, the region immediately after the throat. Since increasing Hartmann number reduces the size of the recirculation zone, the magnitude of the wall shear stress due to the negative velocity in the recirculation zone also decrease in magnitude. This can be seen in Figure 12. As the recirculation zone vanishes at Ha = 30, the magnitude of the shear stress in the recirculation zone decreases significantly which is evident in the red curve, however, at later distance the shear stress increases again due to the increased velocity near the wall.

5. Tools used

Mesh generator: Gmsh
Plot generator: Matplotlib, python
Graphic editor: Inkscape
Flowchart editor: Draw.io
Latex editor: Overleaf

References

Ghahderijani, M. J., Esmaeili, M., Afrand, M., and Karimipour, A. (2017). Numerical simulation of mhd fluid flow inside constricted channels using lattice boltzmann method. *J Appl Fluid Mech*, 10(6):1639–48.

Midya, C., Layek, G., Gupta, A., and Mahapatra, T. R. (2003). Magnetohydrodynamic viscous flow separation in a channel with constrictions. *J. Fluids Eng.*, 125(6):952–962.

Weier, T., Gerbeth, G., Mutschke, G., Lielausis, O., and Lammers, G. (2003). Control of flow separation using electromagnetic forces. *Flow, Turbulence and Combustion*, 71(1-4):5–17.

Nomenclature

η	Magnetic diffusivity, m^2/s
$\mathbf{B_0}$	Applied magnetic field, $Tesla$
$\mathbf{B}$	Total magnetic field, $Tesla$
$\mathbf{V}$	Velocity, m/s
μ	Dynamic viscocity, kg/ms
μ_0	magnetic constant, H/m
ρ	Density, kg/m^3
σ	Electrical conductivity, S/m
d	Height of the constriction, m
H	Width of the constriction, m
L	Length of the channel, m
P	Pressure, N/m^2
Re	Reynolds number
Re_m	Magnetic Reynolds number
w	Width of the channel, m